

"EXTRAPOLATIONS" TO THE Z = 40 - 60 REGION OF ELEMENTS

Ingemar Ragnarsson,  
Department of Mathematical Physics,  
Lund Institute of Technology,  
Lund, Sweden.

Introduction

As a test case for the method of shell parameter extrapolations employed in the superheavy region we have used the same prescriptions to treat the regions below the rare earth region.

These calculations have also great interest in themselves although other systematic calculations, e.g. the ones by Arseniev, Sobiscevski and Soloviev<sup>1)</sup>, have been performed in the fission decay product regions, previously. The calculations described in the present paper are analogous to those of Nilsson, Tsang et al as of ref.<sup>2)</sup> in the rare-earth and actinide regions, They differ from those of ref.<sup>1)</sup> only in three respects

a) we have included the  $P_4$  degree of freedom while neglecting the gamma degree of freedom (the calculations seem to bear out that neither  $P_4$  nor the rotationally asymmetric degree of freedom is a very important degree of freedom in this particular region).

b) the Strutinsky normalisation<sup>3)</sup> is employed throughout our calculations (although for comparison some cases have been studied based on the Bés-Szymanski method).

c) in these calculations we have as a first attempt assumed  $\kappa$  and  $\mu$  to be linear functions in A and the extrapolations have been made from the values of  $\kappa$  and  $\mu$  that have been fitted to data in the rare-earth and actinide regions. In addition different alternative recipes have been

attempted in ref.<sup>1)</sup> and in the present calculations.

### Potential employed

To calculate the single-particle energies and total energies as a function of nuclear distortion we have employed the potential of ref.<sup>2)</sup>

$$V = V_{\text{osc}} + V_{\text{corr}}$$

where

$$V_{\text{osc}} = \frac{1}{2} M \omega_0^2 (\epsilon, \epsilon_4) \cdot \rho^2 \left( 1 - \frac{2}{3} \epsilon P_2(\cos \theta_t) + 2 \epsilon_4 P_4(\cos \theta_t) \right)$$

$$V_{\text{corr}} = - 2 \kappa \hbar \omega_0 \left[ \vec{I}_t \cdot \vec{s} + \mu \left( \vec{I}_t^2 - \langle \vec{I}_t^2 \rangle_N \right) \right]$$

For  $\omega_0$  we have assumed

$$\hbar \omega_0 \begin{pmatrix} N \\ Z \end{pmatrix} = 42 \cdot A^{-1/3} \left( 1 \pm \frac{1}{3} \frac{N-Z}{A} \right) \text{ MeV}$$

where the last condition assumes that the average nuclear volume is proportional to A and that the r.m.s. neutron and proton radii are roughly equal along the nuclear stability line.

These parameters have in the publication cited<sup>2)</sup> been determined from a fit of single-particle levels in the deformed rare-earth and actinide regions to the empirical level order.

### The single-particle calculations

In the whole region ( $40 < Z < 62$ ) calculations have been done with  $\kappa$  and  $\mu$  obtained by linear extrapolation in A from the rare-earth and actinide regions. For  $40 < Z < 48$  also modified values of  $\kappa$  and  $\mu$  have been used. As

seems apparent from fig. 1 where "semiempirical"  $\kappa$  and  $\mu$  values in the regions  $A \approx 25$ ,  $150 < A < 190$ ,  $A > 220$  are given as circles, the linear A-dependence is hardly credible far below the rare earth region. We have therefore alternatively interpolated from the rare earth to the Al-region ("modified parameters") as indicated in fig. 1. Values of  $\kappa$  and  $\mu$  are given in table 1 and single particle level diagrams for extrapolated as well as modified parameters are shown in figs. 2 and 3.

#### The Bés-Szymanski and Strutinsky shell corection methods

Presently we have in these equilibrium calculations applied the shell correction method due to Strutinsky<sup>3)</sup>. Essentially it uses the liquid-drop model for normalisation purposes. In the alternative Bés-Szymanski<sup>4)</sup> method, on the other hand, the single-particle energies are simply added with pairing and Coulomb effects included. The physical finding of constant nuclear density inside of the nuclear surface region is expressed by the condition of the conservation of the volume enclosed by equipotential surfaces. For the  $V_{osc}$  part of the potential this condition can be enforced for all equipotential surfaces simultaneously. As presently the other terms of the potential  $\bar{p}$  are not included in this condition, it is not surprising that for larger<sup>2)</sup> distortions<sup>3,4)</sup> and for moderate distortions of other multipoles<sup>5)</sup> than  $P_2$  (as e.g.  $P_4$ ) the Bés-Szymanski method has been found insufficient unless the number of shells included are limited to a small number of shells. For nuclei heavier than  $A \approx 170$  a calculation by the Bés-Szymanski method gives actually oblate minima deeper than the prolate ones contrary to experimental findings in the heavy rare earth and actinide regions as noticed by C.J. Lamm<sup>6)</sup>. It is easy to see that the peculiarity of the  $\bar{I}_t^2$  term is instrumental in bringing about the undue favouring of the oblate shape.

As in the regions here under investigation the competition between oblate and prolate shapes is very keen, we considered it important to fall back on the Strutinsky method, although in the investigation by Arseniev et al<sup>1)</sup> it was reported that the difference between the results obtained alternatively with the Strutinsky and the Bés-Szymanski methods, as far as equilibrium energies were concerned, were usually below 0.5 MeV in the mass regions  $Z > 50$ ,  $N > 82$ . The difference between the region under study and the rare-earth and actinide regions probably lies in the fact that in this light region the importance of the  $\hat{I}_t^2$  term is relatively small as very modest  $\hat{I}_t^2$  values are involved.

The application of the Strutinsky normalisation is described in detail elsewhere<sup>3)</sup> so we shall only outline its main features. By a smearing function the single-particle level density  $G(e)$ , as obtained from the potential described above, is averaged with the help of essentially a Gaussian function with a range parameter that is of the order of the shell spacing. In this way a new smeared level density function  $g(e)$  is obtained. We then form the difference between just filling the lowest possible energy levels or  $E = \sum_v 2e_v$  and

$$\langle E \rangle = \int g(e) e \, de$$

which latter is obtained from the smeared level density function  $g(e)$ . The difference is a measure of the shell structure involved and is denoted the shell correction function by Strutinsky<sup>3)</sup>

$$\delta E_{\text{shell}} = E - \langle E \rangle$$

Following the Strutinsky recipes, in place of the subtracted averaged energy  $\langle E \rangle$  the liquid-drop model energy,  $E_{\text{L.D.}}$ , is substituted. Finally a fluctuating pairing energy term

$$\delta E_{\text{pair}} = E_{\text{PAIR}} - \langle E_{\text{PAIR}} \rangle$$

is added giving

$$E_{\text{tot}} = \delta E_{\text{shell}} + E_{\text{L.D.}} + \delta E_{\text{pair}}$$

Minimum of  $E_{\text{tot}}$  is then determined with respect to the distortion parameters  $\epsilon$  and  $\epsilon_4$ .

The term  $E_{\text{pair}}$  is evaluated by the straight-forward BCS method. The pairing matrix elements  $G_n$  and  $G_p$  are assumed proportional to surface area,  $A_S$  for  $\langle E_{\text{PAIR}} \rangle$  we assume this term to be given by its value at equilibrium distortion. Contrary to other authors we do not assume this term deformation dependent.

#### Pairing calculation. Comparisons of $\Delta$ and total mass with data

In the treatment of the pairing energy we have followed the recipes developed in ref.<sup>2)</sup>. We have used a number of neutron and proton levels above and below the Fermi surface (for no pairing) of  $\sqrt{10} N$  and  $\sqrt{10} Z$ ; because of the smaller number of particles we are forced to make this change from ref.<sup>2)</sup>. Subsequently we must also redetermine the pairing strength parameter, for which we have assumed an isospin dependence

$$G_n \cdot A = g_n^0 + g_n^1 \frac{N-Z}{A}$$

$$G_p \cdot A = g_p^0 + g_p^1 \frac{N-Z}{A}$$

Note that we have relaxed the conditions  $g_n^1 = -g_p^1$  assumed in ref.<sup>1)</sup> expected to hold for  $N \approx Z$  and the limit that the Coulomb energy being negligible. For lighter nuclei we should expect this relation to be approached.

The  $G$  values are determined by fitting the theoretical  $\Delta$  to the experimental odd-even mass difference. This comparison is exhibited in figs. 7a and b. The values of  $g^0$  and  $g^1$  which we have used are also given there. It must be pointed out that when the distances between the energy levels near the Fermi surface is not small compared to  $\Delta$ , the comparison above is somewhat incorrect. Therefore the fit of  $\Delta_p$  must be made essentially when  $Z$  is not too near to 50 and the fit of  $\Delta_n$  when  $N$  is not too near to 50 and 82. We then find that for the  $G$ -values corresponding to the linearly extrapolated  $\kappa$  and  $\mu$  the isospin dependence is too great but that the fit on the average is rather good. However, just a small change of  $G$  will change  $\Delta$  considerably and in the investigations by Arseniev et al<sup>1)</sup> it is reported that such a great change of  $G$  as 10% will, as a rule, change the  $\epsilon$ -values of the minima by less than 0.01. Therefore, if  $G$  is modified to better fit  $\Delta$  to the even-odd mass differences, the equilibrium distortions will be negligibly affected. For the modified  $\kappa$  and  $\mu$  values the  $G$  values have been re-determined. We also find that the fit is better, especially for the protons.

In fig. 8 the difference between the experimental and theoretical nuclear masses are plotted. The differences are of the same order as for the heavier nuclei, in fact they are better for the modified  $\kappa$  and  $\mu$  values than for the linearly extrapolated ones. It can be noticed that for the magic neutron number 82, the theoretical mass is too small. For greater  $N$  values this discrepancy between theoretical and experimental masses disappears. This appears to make it probable that the theoretical  $N=82$  gap in the energy levels is too great.

### Results of calculations

In figs. 4a, b and c some typical total energy surfaces are shown in the  $(\epsilon, \epsilon_4)$ -plane. In figs. 5a and b the  $\epsilon$ - and  $\epsilon_4$ -coordinates of the minima are given. These values as well as the depths of the minima are tabulated in table 2. One may notice that for the linearly extrapolated parameters the prolate minimum is nearly always the deepest one while the modified  $\kappa$  and  $\mu$ -values give rise to a dominance of oblate distortions, at least for the nuclei which can be expected to be permanently deformed. We estimate roughly that the deformation is permanent when the energy of the deepest minimum is at least about 0.5 MeV smaller than the energy at spherical shape. The depths of the minima can be studied in figs. 6a, b, c and d.

### Comparison with data

A large number of new data in the deformed region have recently become available for neutron rich even-even isotopes of  $^{40}\text{Zr}$ ,  $^{42}\text{Mo}$ ,  $^{44}\text{Ru}$  and  $^{46}\text{Pd}$ . Usually only the  $2 \rightarrow 0$  and  $4 \rightarrow 2$  rotational transitional energies are determined empirically. The  $E_{4^+}/E_{2^+}$  ratio is in excess of 3 only in two of the nuclei studied. Some of these spectra still indicate stable distortions. From the gamma half-life one can also deduce the  $B(E2)$  value or  $Q_0$ . We list in table 2 the experimental  $E_{2^+}$ ,  $E_{4^+}/E_{2^+}$ , and  $|Q_0|$  values as given by Cheifetz, Jared, Thompson, and Wilhelmy<sup>7)</sup>. Corresponding values of deformation energies and  $Q_0$  for the theoretical prolate and oblate cases are given in the same table for the two alternative sets of  $\kappa$  and  $\mu$ .

First it is found that the correlation between empirically low excitation energies of the  $2^+$  states and large theoretical deformation

energies (deep minima) is rather good. The transition point between spherical and deformed equilibrium distortions can be decided first when the vibrational energies are added. As a semiempirical rule it appears that we must require for stable distortions that the energy of the deepest minimum be at least 1 - 1.5 MeV smaller than the energy of spherical shape. (Note that in drawing figs 5a and b we used 0.5 MeV as the threshold.) With this rule we conclude for the modified  $\kappa$  and  $\mu$  values that the isotopes from  $^{100}\text{Zr}$ ,  $^{104}\text{Mo}$  ( $^{102}\text{Mo}$ ), and  $^{108}\text{Ru}$  ( $^{106}\text{Ru}$ ) and on are permanently deformed. If any Pd-isotopes are permanently deformed is unclear by this requirement. For the linearly extrapolated  $\kappa$  and  $\mu$  parameters the deformations are greater than for the modified parameters. This is the case especially for the Zr-isotopes where the theoretical results for the extrapolated parameters appear to be clearly incorrect. This is, however, reasonable as we are there farthest away from the rare-earth region and it is more probable that the linear extrapolation is no longer satisfactory.

When it comes to a detailed comparison of the magnitudes of the theoretical and experimental  $Q_0$  values, one notices that the former are usually only of the order of 60 - 80 % of the latter for the well deformed nuclei for both sets of  $\kappa$  and  $\mu$ . This discrepancy between theory and experiment for nuclei exhibiting rotational spectra is much in excess of the discrepancy encountered in the rare-earth and actinide regions of nuclei. Conceivably this can be remedied by a modification of the unknown single-particle scheme (although this hardly seems probable). As the distortion estimates obtained by the B.-S. and the Strutinsky methods of calculation give results that here are in rather poor agreement with each other, the B.-S. method giving the better results, one might be tempted to question the local applicability of the parameters of the liquid-drop model entering through the Strutinsky method. Particularly sensitive is the surface energy term. Here the sharing of strength between



the isospin independent surface energy and surface symmetry energy terms is fixed in advance for the Mayer-Swiatecki<sup>8)</sup> liquid-drop parameter set here employed. In the M.S. parameter choice the total strength is determined by a fit to the masses along the stability line of the mass valley. The heavy region is in this fit given particular weight. The fission decay products are far off the stability line and a deficiency in the surface symmetry term might then exhibit itself and conceivably explain some of the discrepancy in the  $Q_0$ -values.

Therefore we have increased this term by a factor 3 and calculated the new  $(\epsilon, \epsilon_4)$ -values of the minima. We find (see fig. 9) that in most cases the  $\epsilon$ -values of the minima are changed not more than 0.01 - 0.03, which is not enough to get the theoretical  $Q_0$  as large as the experimental ones.

As indicated above we have also performed a calculation without the use of the Strutinsky normalisation. Also for this case we have calculated the  $(\epsilon, \epsilon_4)$ -values of the minima. On the prolate side the change is not significant while on the oblate side the  $\epsilon$ -values of the minima might be changed as much as 0.10 (see fig. 9 and 10). If we do not use the Strutinsky method the tendency for oblate distortions is increased and we find for both of the regions,  $Z < 50$  and  $Z > 50$ , that the oblate minima in most cases are the deepest ones. We also find that in some cases the  $\epsilon_4$ -distortions are very much affected by the Strutinsky normalisation. (This parallels the results of P. Möller<sup>5)</sup> in the rare-earth region.)

## Conclusions

It appears that a new deformed region is well established experimentally with the study of the neutron rich light fission products. This region of distortion is well brought out by the theoretical calculations. The magnitude of the distortions are less well reproduced and it is speculated that some of the discrepancy may be due to the Strutinsky method of calculation or rather the liquid drop parameters entering into the theoretical calculations through the employment of the Strutinsky shell correction method.

## Acknowledgements

For guidance and most generous help the author wishes to express his deep gratitude to Professor S.G. Nilsson, who suggested this investigation. I also wish to thank all members at the Department of Mathematical Physics in Lund, especially P. Möller for generous access to computer programs. Comments on the work by Professor B. Mottelson are gratefully acknowledged.

References

1. D.A. Arseniev, A. Sobiczewski and V.G. Soloviev, Nucl. Phys. A 126 (1969) 15
2. S.G. Nilsson, C.F. Tsang, A. Sobiczewski, Z. Szymanski, S. Wycech, C. Gustafsson, I.-L. Lamm, P. Möller, B. Nilsson, Nucl. Phys. A131 (1969) 1
3. V.M. Strutinsky, Nucl. Phys. A95 (1967) 420
4. D.R. Bés and Z. Szymanski, Nucl. Phys. 28(1961) 42  
Z. Szymanski, Nucl. Phys. 28(1961) 63
5. P. Möller, Nucl. Phys. A142 (1970) 1
6. C.J. Lamm, private communication
7. E. Cheifetz, R.C. Jared, S.G. Thompson and J.B. Wilhelmy, Experimental information concerning deformation of neutron rich nuclei in the  $A \approx 100$  region, Univ. of Calif., Lawrence Radiation Report, UCRL-19584 (April 1970), Phys.Rev.Letters 25(1970)38
8. W.D. Myers and W.J. Swiatecki, Nucl. Phys. 81(1966) 1

Table captions

- Table 1 Values of  $\kappa$  and  $\mu$  employed in the single-particle calculation corresponding to different regions of mass.
- Table 2a The coordinates and corresponding intrinsic quadrupole moments of the oblate  $(\epsilon_0^-, (\epsilon_4)_0^-, Q_0^-)$  and prolate minimum  $(\epsilon_0^+, (\epsilon_4)_0^+, Q_0^+)$  for  $Z=54, 56, 58, 60$  and  $62$ .  $E^+$  is the depth of the prolate minimum and  $\Delta E$  is the difference in depth between the oblate and prolate minimum. If  $\Delta E > 0$  the prolate minimum is the deepest one. Linearly extrapolated  $\kappa$  and  $\mu$  values have been used.
- Table 2b Same as table 2a for  $Z=40, 42, 44, 46$  and  $48$ . The results are given for linearly extrapolated as well as modified  $\kappa$  and  $\mu$  values.
- Table 3 Experimental results taken from ref<sup>7)</sup> compared to theory.  $E_{\max}$  is the deepest minimum. The quadrupole moments corresponding to both minima are given, for the deepest minimum no parenthesis is used.

Table 1

A	Protons		Neutrons		
	$\kappa$	$\mu$	$\kappa$	$\mu$	
25	0.08	0	0.08	0	Fitted to the experimental energy levels
165	0.0637	0.600	0.0637	0.420	
242	0.0577	0.650	0.0635	0.325	
140	0.0657	0.584	0.0637	0.451	Extrapolated from A = 165 and A = 242
122	0.0671	0.572	0.0638	0.493	
103	0.0686	0.560	0.0638	0.497	
110	0.070	0.40	0.066	0.35	Interpolated from A = 165 to A = 25

Table 2a

	$Q_0^-$			$Q_0^+$			$E^+$ (MeV)	$\Delta E$ (MeV)
	$\epsilon_0^-$	$(\epsilon_4)_0^-$	(fm <sup>2</sup> )	$\epsilon_0^+$	$(\epsilon_4)_0^+$	(fm <sup>2</sup> )		
<sup>116</sup> Xe	-0.16	-0.01	-224	0.20	-0.01	332	0.8	0.4
<sup>118</sup> Xe	-0.18	-0.01	-246	0.21	0.00	349	0.9	0.3
<sup>120</sup> Xe	-0.19	0.00	-260	0.21	0.01	358	1.1	0.2
<sup>122</sup> Xe	-0.18	0.00	-260	0.20	0.01	335	1.0	0.0
<sup>124</sup> Xe	-0.18	0.01	-253	0.17	0.01	293	0.8	-0.1
<sup>126</sup> Xe	-0.15	0.01	-218	0.14	0.01	234	0.7	-0.1
<sup>144</sup> Xe	-0.14	-0.03	-226	0.16	-0.06	322	2.0	1.0
<sup>120</sup> Ba	-0.20	-0.01	-293	0.25	0.00	450	2.1	0.7
<sup>122</sup> Ba	-0.20	-0.01	-298	0.25	0.01	456	2.2	0.6
<sup>124</sup> Ba	-0.20	0.00	-294	0.24	0.02	431	2.1	0.3
<sup>126</sup> Ba	-0.20	0.01	-295	0.20	0.01	360		0.1
<sup>128</sup> Ba	-0.19	0.01	-284	0.19	0.02	337	1.3	0.0
<sup>130</sup> Ba	-0.15	0.02	-226	0.24	0.01	253	0.8	0.0
<sup>144</sup> Ba	-0.13	-0.03	-217	0.11	-0.04	220	0.8	0.3
<sup>124</sup> Ce	-0.23	0.00	-346	0.28	0.01	537	3.2	1.1
<sup>126</sup> Ce	-0.22	0.00	-340	0.27	0.02	520	3.0	0.8
<sup>128</sup> Ce	-0.22	0.01	-331	0.24	0.02	466	2.5	0.4
<sup>130</sup> Ce	-0.20	0.01	-310	0.20	0.02	378	2.0	0.2
<sup>132</sup> Ce	-0.18	0.02	-279	0.18	0.02	339	1.2	0.1
<sup>134</sup> Ce	-0.12	0.02	-195	0.10	0.01	188	0.5	0.0
<sup>146</sup> Ce	-0.14	-0.03	-256	0.14	-0.04	303	1.0	0.4
<sup>148</sup> Ce	-0.19	-0.04	-330	0.20	-0.06	456	3.3	1.5
<sup>132</sup> Nd	-0.22	0.02	-346	0.23	0.02	454	2.5	0.5
<sup>134</sup> Nd	-0.20	0.02	-323	0.20	0.02	397	1.7	0.3
<sup>136</sup> Nd	-0.14	0.02	-244	0.14	0.02	276	0.7	0.0
<sup>148</sup> Nd	-0.15	-0.03	-276	0.17	-0.04	382	1.2	0.5
<sup>150</sup> Nd	-0.19	-0.03	-357	0.20	-0.05	475	3.6	1.8
<sup>138</sup> Sm	-0.16	0.02	-285	0.18	0.02	365	0.9	0.1
<sup>140</sup> Sm	-0.10	0.02	-181	0.08	0.01	162	0.1	-0.1
<sup>150</sup> Sm	-0.15	-0.03	-281	0.18	-0.04	425	1.3	0.6
<sup>152</sup> Sm	-0.20	-0.03	-378	0.21	-0.04	515	3.6	1.8
<sup>154</sup> Sm	-0.20	-0.03	-385	0.23	-0.04	566	6.0	3.2
<sup>156</sup> Sm	-0.21	-0.02	-408	0.24	-0.04	611	7.9	4.4
<sup>158</sup> Sm	-0.22	-0.02	-424	0.26	-0.02	646	9.6	5.4

Table 2b

	Lin. extr. $\kappa$ and $\mu$						Mod. $\kappa$ and $\mu$							
	$\epsilon_0^-$	$(\epsilon_4)_0^-$	$Q_0^-$ (fm <sup>2</sup> )	$\epsilon_0^+$	$(\epsilon_4)_0^+$	$Q_0^+$ (fm <sup>2</sup> )	$\epsilon_0^-$	$(\epsilon_4)_0^-$	$Q_0^-$ (fm <sup>2</sup> )	$\epsilon_0^+$	$(\epsilon_4)_0^+$	$Q_0^+$ (fm <sup>2</sup> )	$E^+$ (MeV)	$\Delta E$ (MeV)
<sup>98</sup> Zr	-0.23	-0.01	-204	.25	-0.00	288	-0.21	-0.00	-185	.17	.00	186	0.24	-0.38
<sup>100</sup> Zr	-0.26	-0.01	-233	.30	.00	357	-0.26	-0.01	-230	.28	.00	326	0.92	-0.61
<sup>102</sup> Zr	-0.27	.00	-245	.30	.01	358	-0.26	.01	-233	.30	.01	353	1.68	-0.50
<sup>104</sup> Zr	-0.28	.02	-248	.30	.02	357	-0.26	.02	-230	.30	.02	358	2.07	-0.56
<sup>106</sup> Zr							-0.26	.04	-233	.30	.04	358	2.44	-0.76
<sup>108</sup> Zr							-0.27	.05	-238	.30	.05	357	2.55	-1.03
<sup>110</sup> Zr							-0.27	.06	-238	.30	.07	357	2.22	-1.25
<sup>100</sup> Mo	-0.20	.00	-191	.20	.00	235	-0.18	.00	-175	.15	-0.00	172	0.31	0.01
<sup>102</sup> Mo	-0.23	.00	-224	.25	.00	312	-0.24	.00	-226	.21	.00	245	0.66	-0.38
<sup>104</sup> Mo	-0.25	.01	-240	.28	.01	348	-0.25	.01	-236	.26	.01	322	1.16	-0.56
<sup>106</sup> Mo	-0.26	.03	-246	.29	.02	360	-0.25	.03	-237	.27	.02	340	1.48	-0.75
<sup>108</sup> Mo	-0.26	.04	-250	.29	.04	369	-0.26	.04	-244	.28	.03	351	1.79	-1.04
<sup>110</sup> Mo	-0.26	.05	-249	.29	.06	370	-0.26	.06	-249	.28	.05	357	1.83	-1.39
<sup>112</sup> Mo							-0.26	.06	-250	.28	.06	350	1.46	-1.68
<sup>102</sup> Ru	-0.17	.00	-173	.18	-0.00	218	-0.10	-0.00	-106	.15	-0.00	181	0.55	0.40
<sup>104</sup> Ru	-0.21	.01	-212	.20	.00	251	-0.18	.00	-190	.18	.00	224	0.85	0.37
<sup>106</sup> Ru	-0.23	.02	-236	.23	.01	298	-0.23	.01	-238	.20	.01	258	1.11	0.00
<sup>108</sup> Ru	-0.24	.03	-247	.25	.02	322	-0.24	.02	-242	.22	.01	288	1.29	-0.31
<sup>110</sup> Ru	-0.25	.04	-255	.26	.03	342	-0.25	.04	-250	.23	.02	305	1.49	-0.67
<sup>112</sup> Ru	-0.25	.05	-256	.26	.05	344	-0.26	.05	-258	.23	.03	301	1.47	-1.02
<sup>114</sup> Ru							-0.26	.06	-259	.20	.02	201	1.33	-1.06





Table 3

		Experimental results 7)		Lin. extr. $\kappa$ and $\mu$		Mod. $\kappa$ and $\mu$	
$E_{2^+}$ (keV)	$E_{4^+}/E_{2^+}$	$ Q_0 $ (fm <sup>2</sup> )	$E_{\max}$ (MeV)	$Q_0$ (fm <sup>2</sup> )	$E_{\max}$ (MeV)	$Q_0$ (fm <sup>2</sup> )	
<sup>96</sup> Zr	1740		0.75		0.01		
<sup>98</sup> Zr	1223		1.80		0.62		
<sup>100</sup> Zr	213	2.65	3.42	343	1.54	(326)	-230
<sup>102</sup> Zr	152	3.15	4.47	575	2.18	(353)	-233
<sup>98</sup> Mo	787		0.43		0.06		
<sup>100</sup> Mo	536		1.31		0.31		
<sup>102</sup> Mo	296	>348	2.36		1.04	(245)	-226
<sup>104</sup> Mo	192	2.92	3.33	465	1.72	(322)	-236
<sup>106</sup> Mo	172	3.04	3.99	467	2.23	(340)	-237
<sup>104</sup> Ru	358		1.65		0.85		
<sup>106</sup> Ru	269		2.33		1.11		
<sup>108</sup> Ru	242	2.75	2.84	384	1.60	(288)	-242
<sup>110</sup> Ru	241	2.76	3.43	382	2.16	(305)	-250
<sup>112</sup> Ru	237	2.73	3.78	426	2.49	(301)	-258
<sup>108</sup> Pd	434		1.39		1.03		
<sup>110</sup> Pd	374		1.73		1.16		
<sup>112</sup> Pd	349	>234	2.14		1.31	271	(-227)
<sup>114</sup> Pd	333	>262	2.30	292	1.34	(273)	-242
<sup>116</sup> Pd	341	>247	2.32	275	1.24	262	(-243)

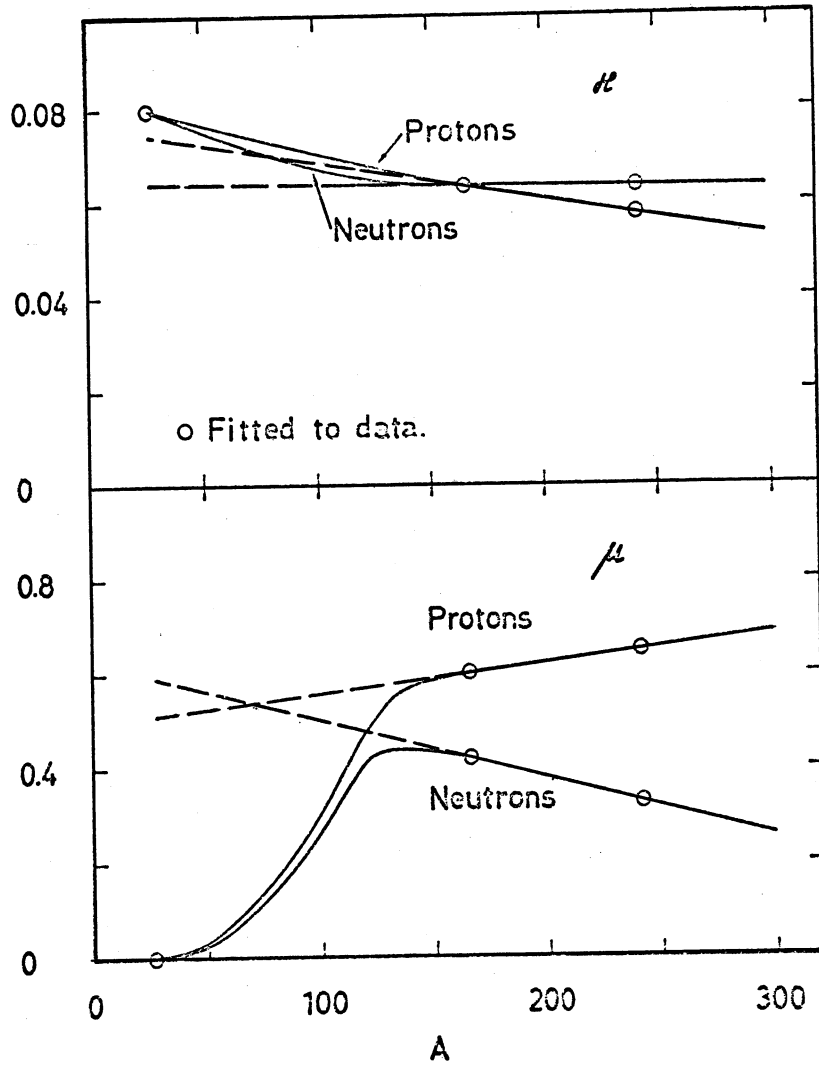


Fig. 1 The variation of  $\kappa$  and  $\mu$  with the mass value A. For A = 165 and 242 the values have been chosen to fit the experimental energy levels as well as possible. For A = 25 the parameters are also considered to be known. To find the  $\kappa$  and  $\mu$  values for A  $\approx$  90-150 we have used two recipes, first a linear extrapolation from the heavier regions and secondly an interpolation between the rare-earth and Al regions ("modified parameters") as shown in the figure.

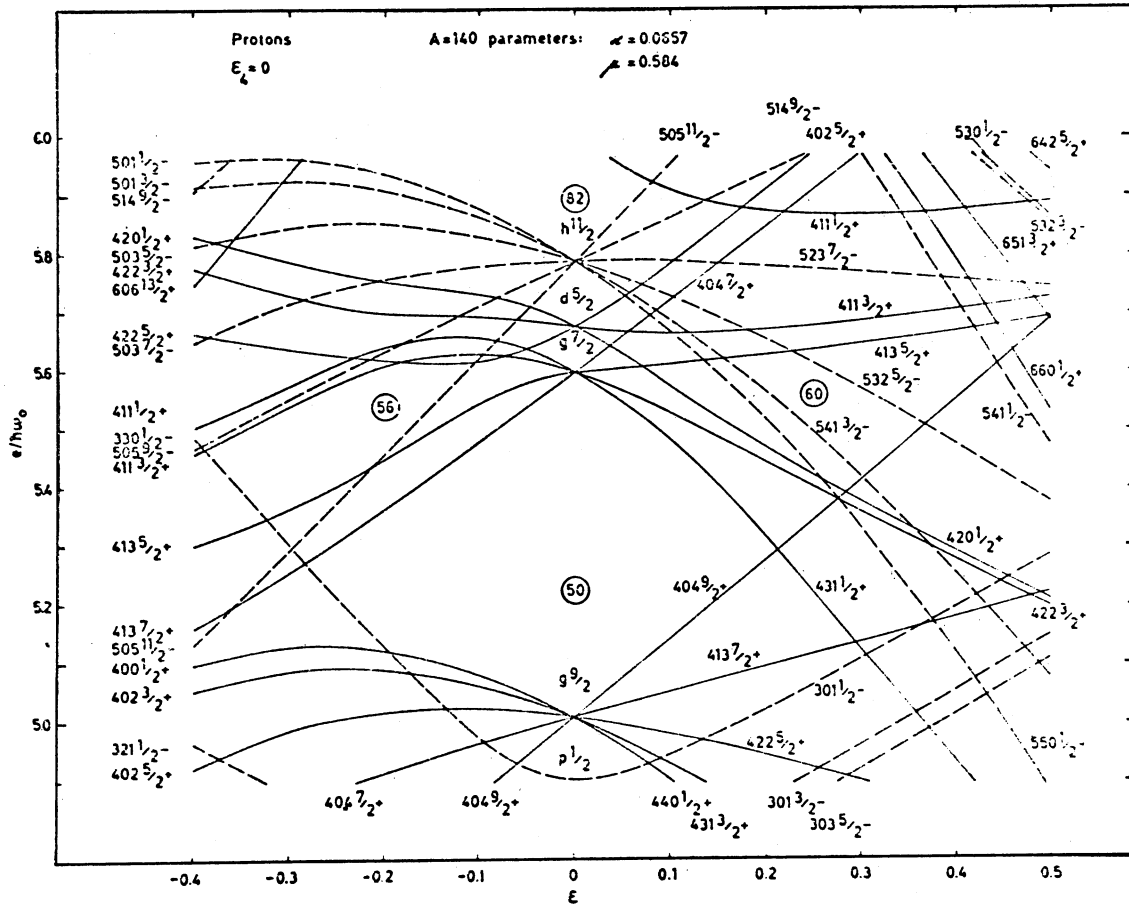


Fig. 2a Single-proton levels for  $A \approx 140$  and linearly extrapolated  $\kappa$  and  $\mu$  values. The levels are assigned asymptotic quantum numbers. Solid lines mark even parity while dashed lines represent odd parity. ( $\epsilon_4 = 0$  is assumed in this figure.)

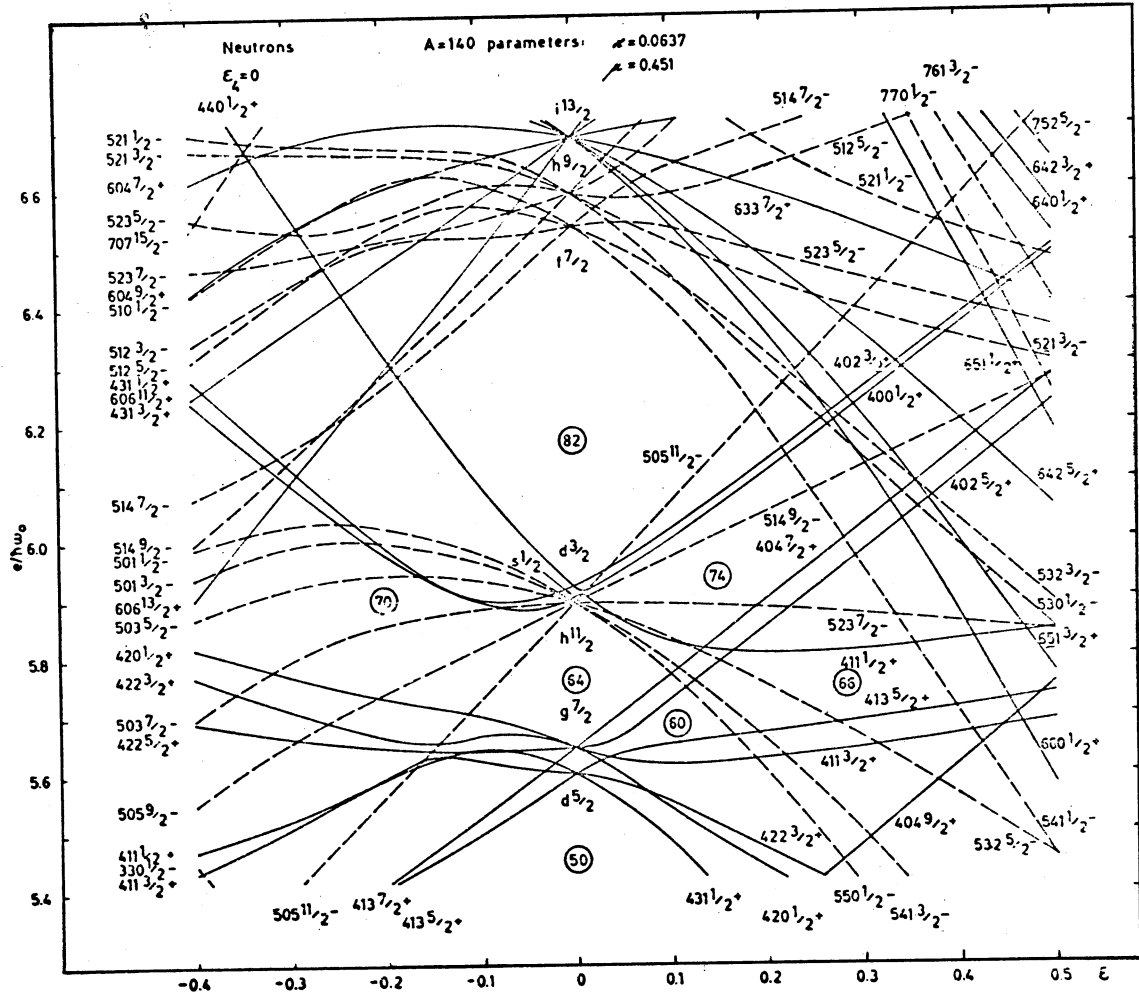


Fig. 2b Single-neutron levels for  $A \approx 140$  based on linearly extrapolated  $\kappa$  and  $\mu$  parameters. ( $\epsilon_4 = 0$ )

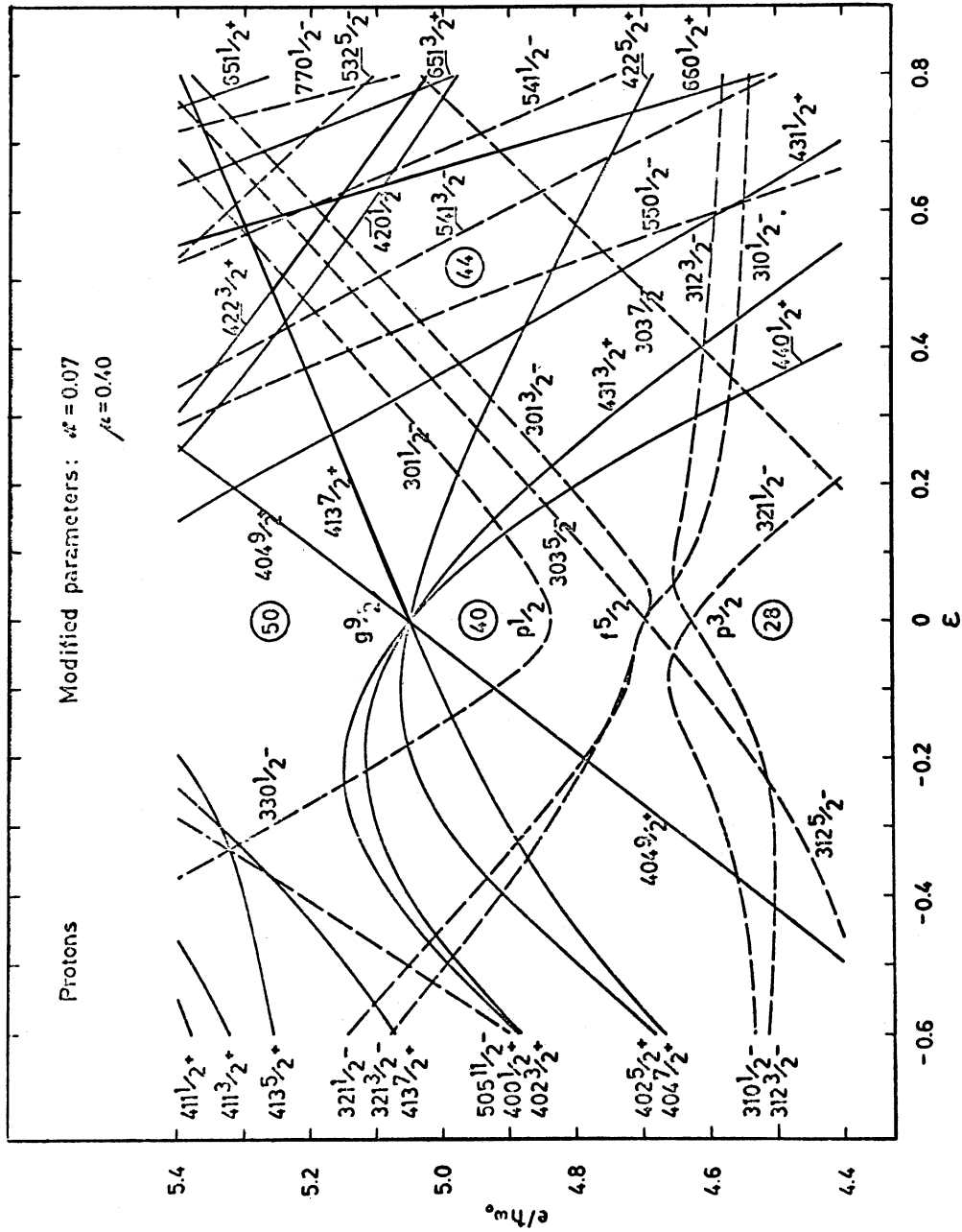


Fig. 3a Single-proton levels for the modified parameters.  $A \approx 110$ . ( $\epsilon_4 = 0$ )

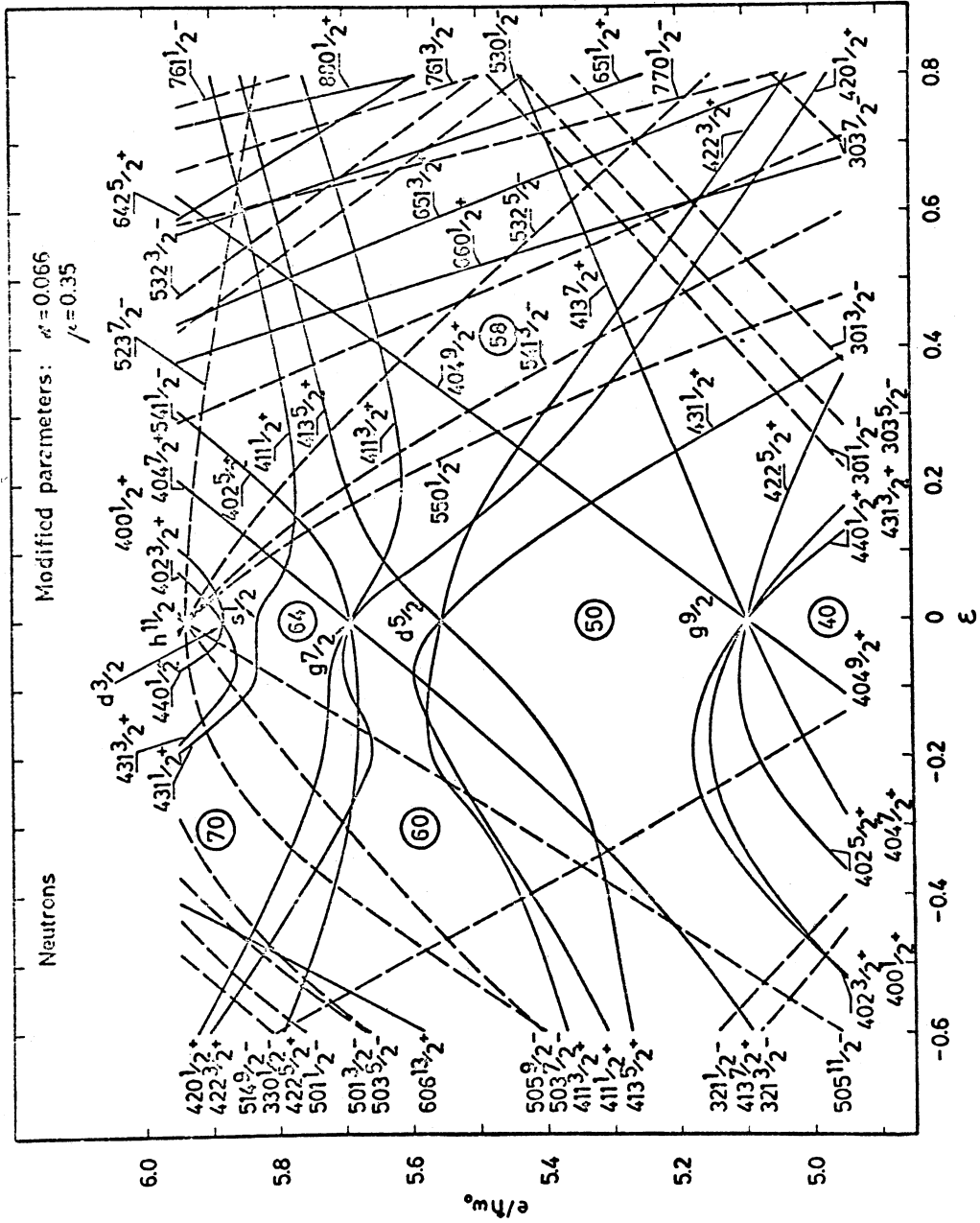


Fig. 3b Single-neutron levels for the modified parameters.  $A=110$  ( $\epsilon=0$ )

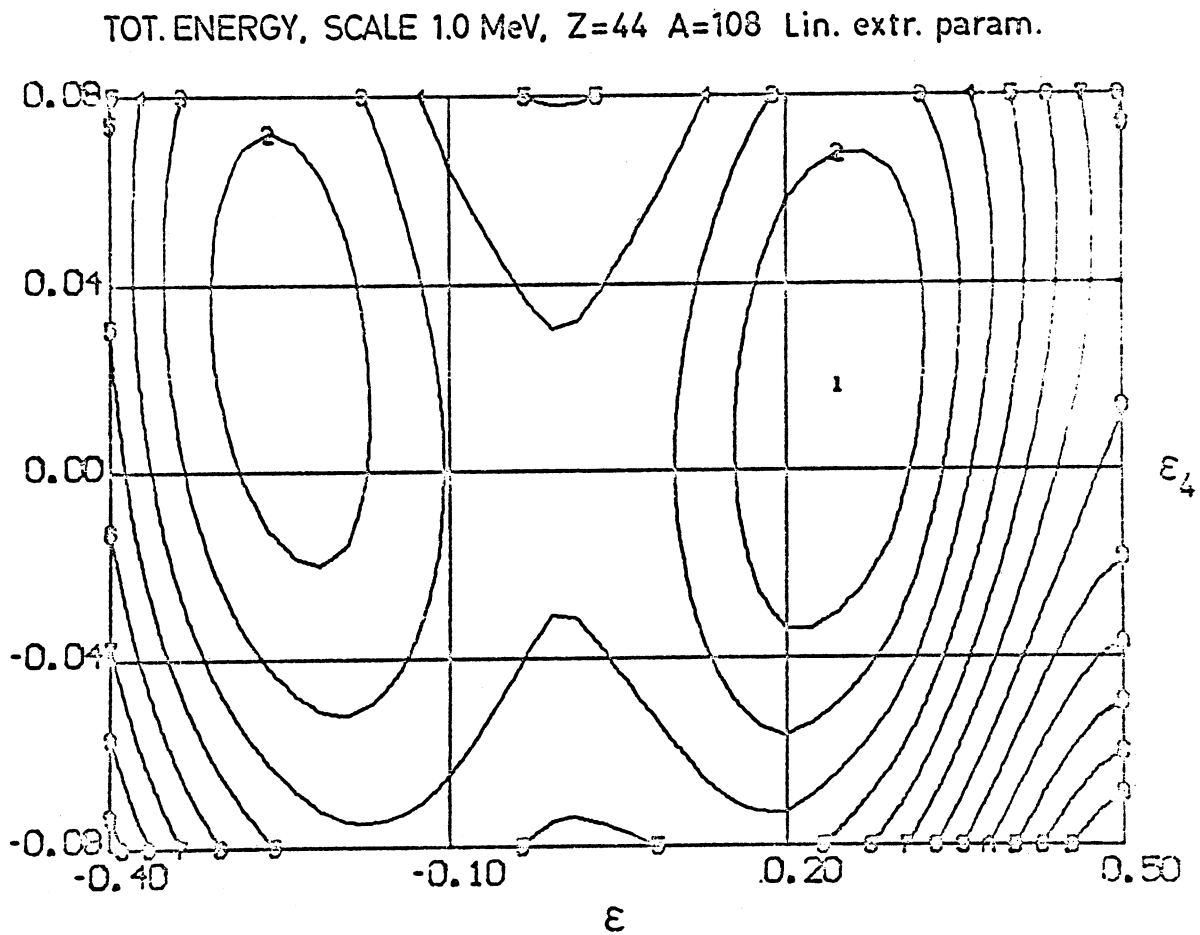


Fig. 4a The total energy surface in the  $(\epsilon, \epsilon_4)$ -plane for  $^{108}_{44}\text{Ru}$ . The  $\kappa$  and  $\mu$  values are linearly extrapolated from rare-earth and actinide regions. The lines represent steps of 1 MeV. The prolate minimum is 0.4 MeV deeper than the oblate one.

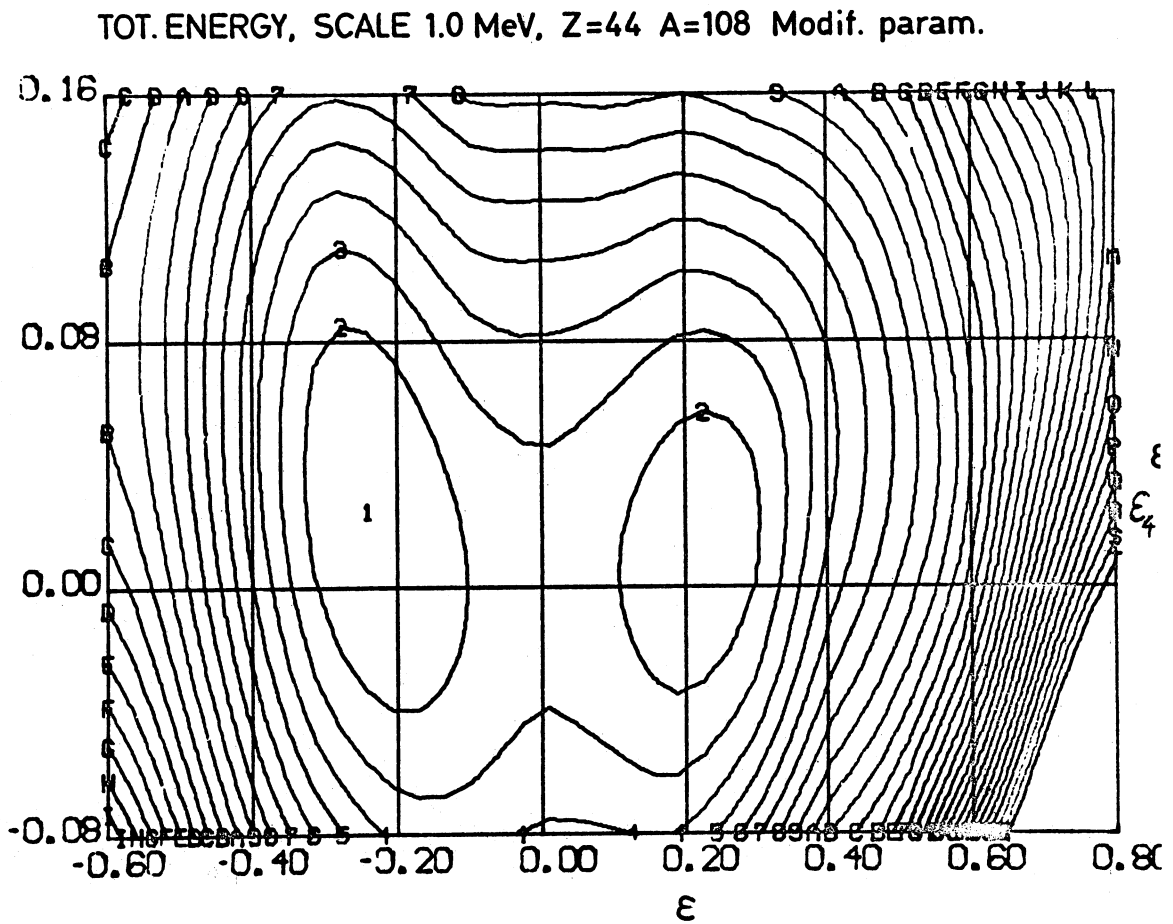


Fig. 4b Same as fig. 4a except that the  $\kappa$  and  $\mu$  values are interpolated between the Al and rare-earth regions and the pairing strength  $G$  is correspondingly changed. The oblate minimum is found to be 0.3 MeV deeper than the prolate one.



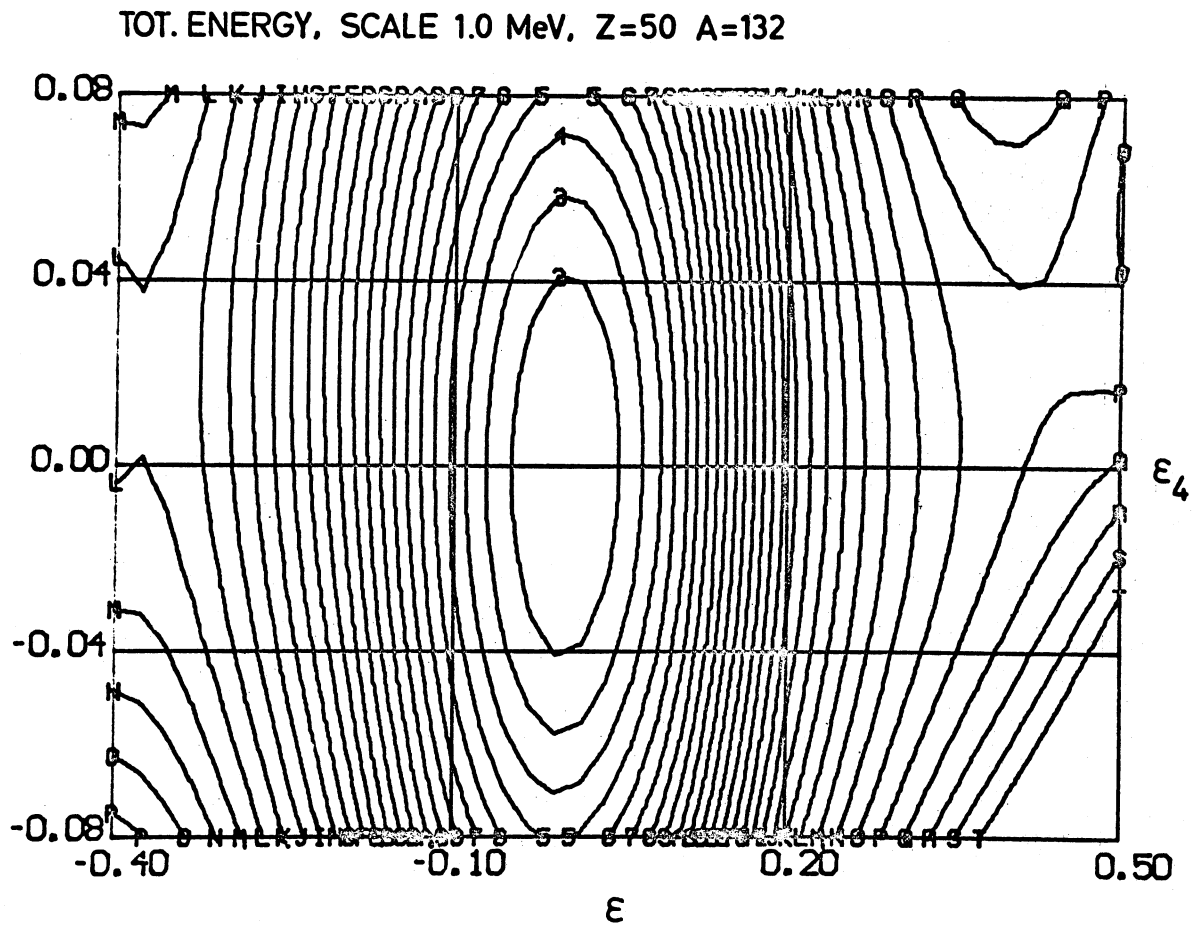


Fig. 4c Same as fig. 4a for the double-magic nucleons  $^{132}_{50}\text{Sn}$

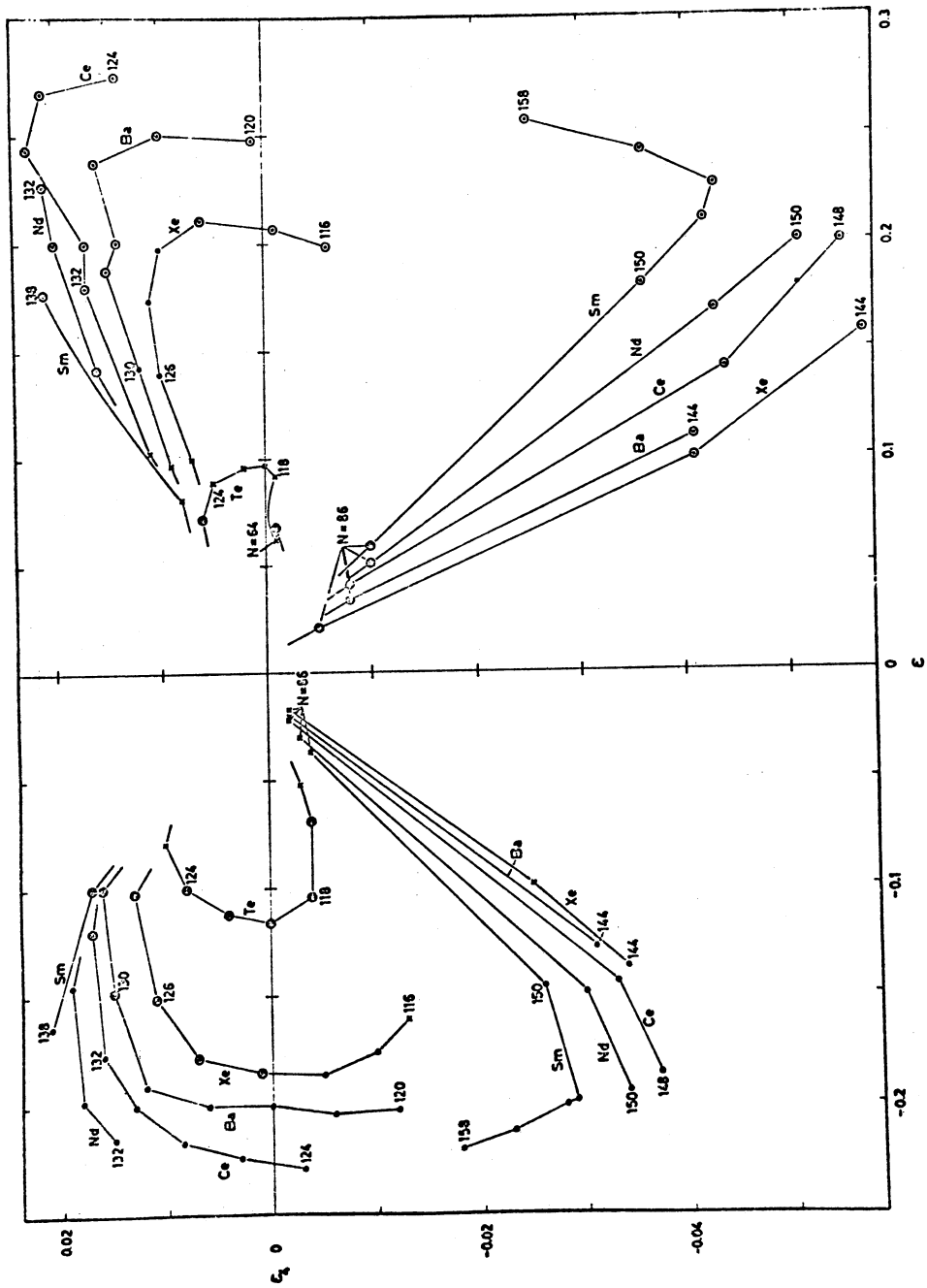


Fig. 5a The minima of the total energy plotted in the  $(\epsilon, \epsilon_4)$ -plane for  $Z=52, 54, 56, 58, 60$ , and  $62$ . For each nucleus the lowest minimum is marked by a circle. In the case that the energy of a minimum differs from the spherical-shape energy by less than  $0.5$  MeV it is marked by a cross, if it differs by more than  $0.5$  MeV it is marked by a point. The  $\kappa$  and  $\mu$  values used are linearly extrapolated ones.



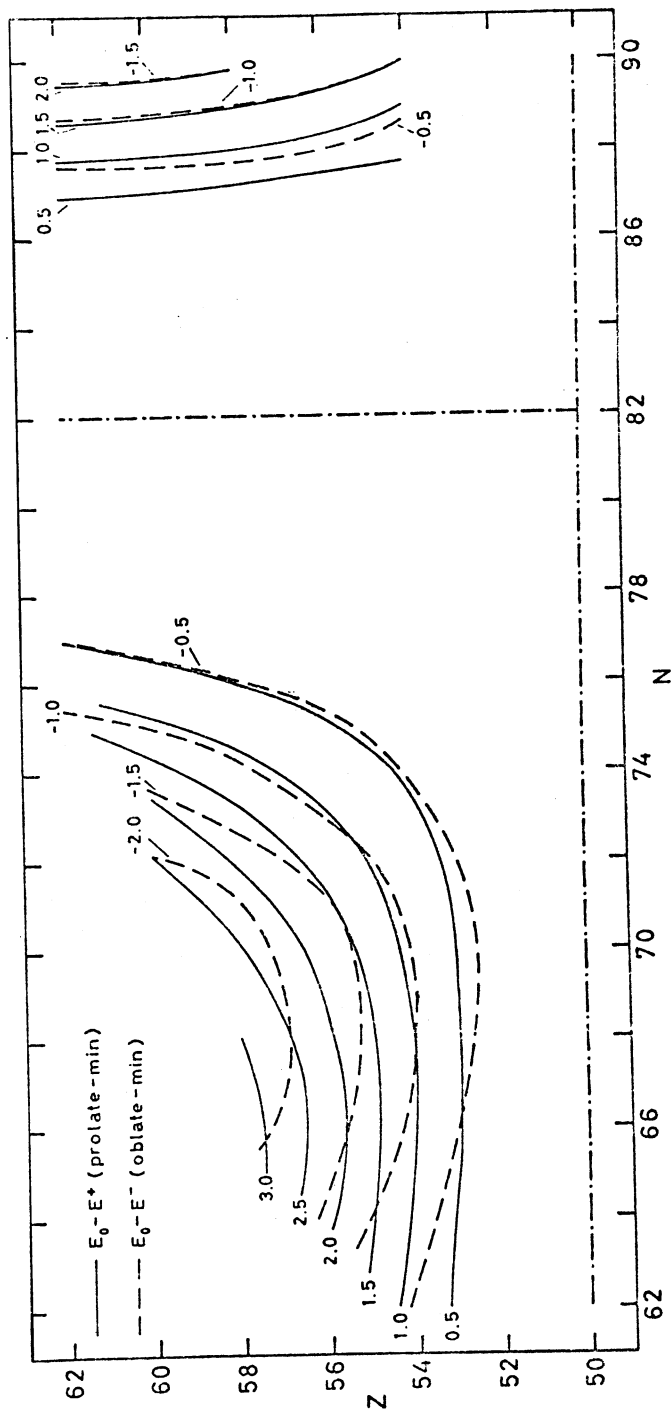


Fig. 6a Contours in the  $(N, Z)$ -plane for the depths of the prolate and oblate minima. Linearly extrapolated values of  $\kappa$  and  $\mu$  are used.

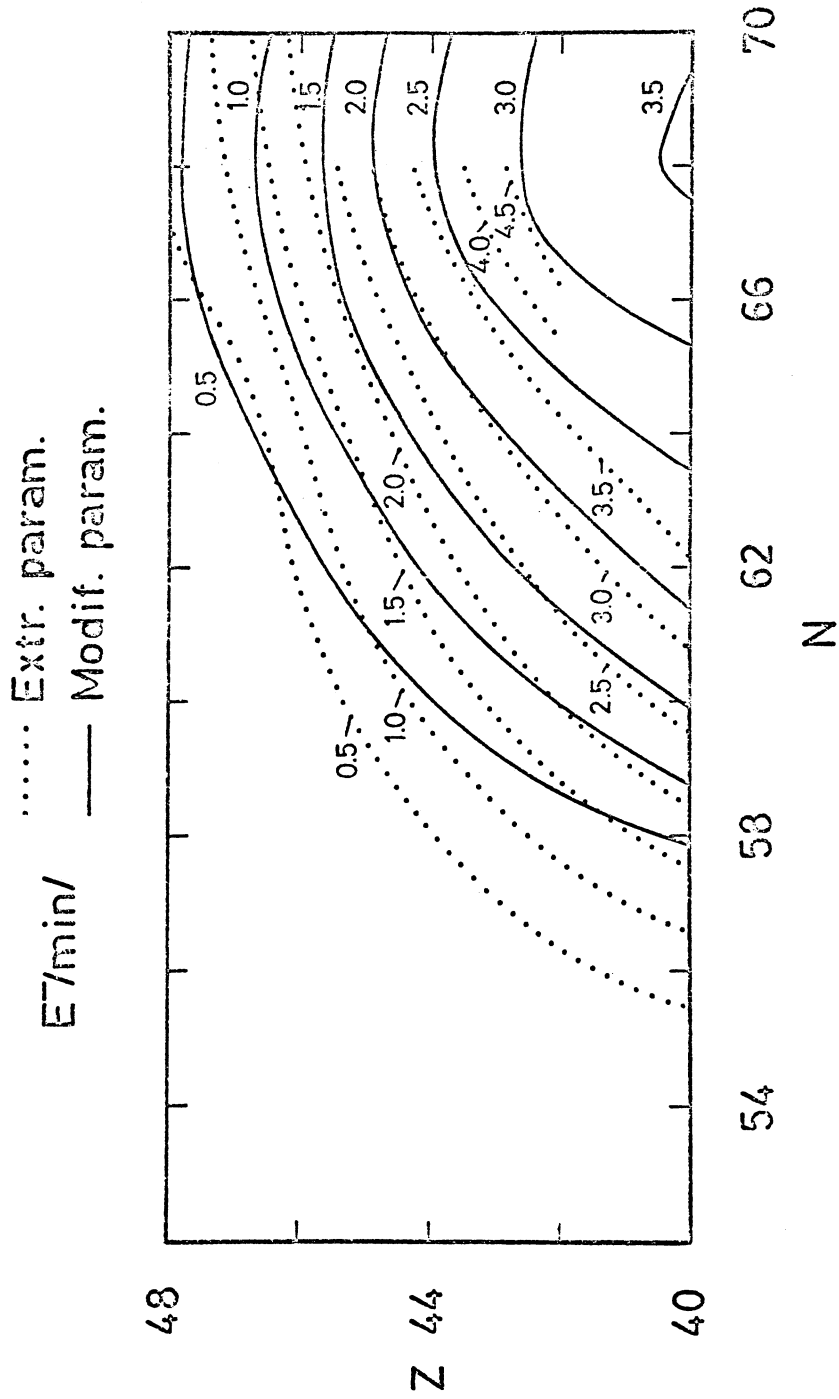


Fig. 6b Contours in the  $(N,Z)$ -plane for the depths of the oblate minima. For the dotted lines  $\kappa$  and  $\mu$  are linearly extrapolated while for the solid lines modified parameters have been used.

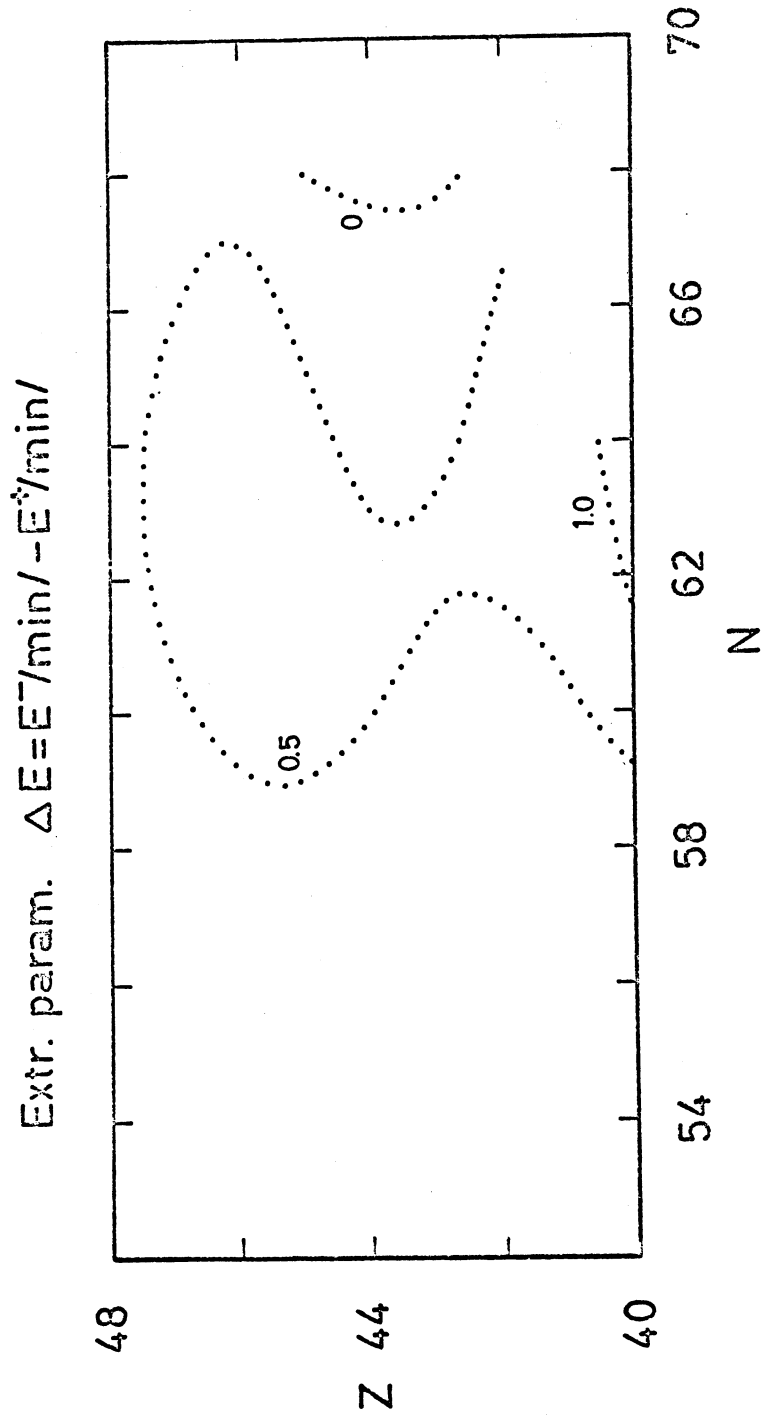


Fig. 6c Contours for the difference in depth between the oblate and prolate minima.  $\kappa$  and  $\mu$  are linearly extrapolated. If  $\Delta E > 0$  the prolate minimum is the deepest one.

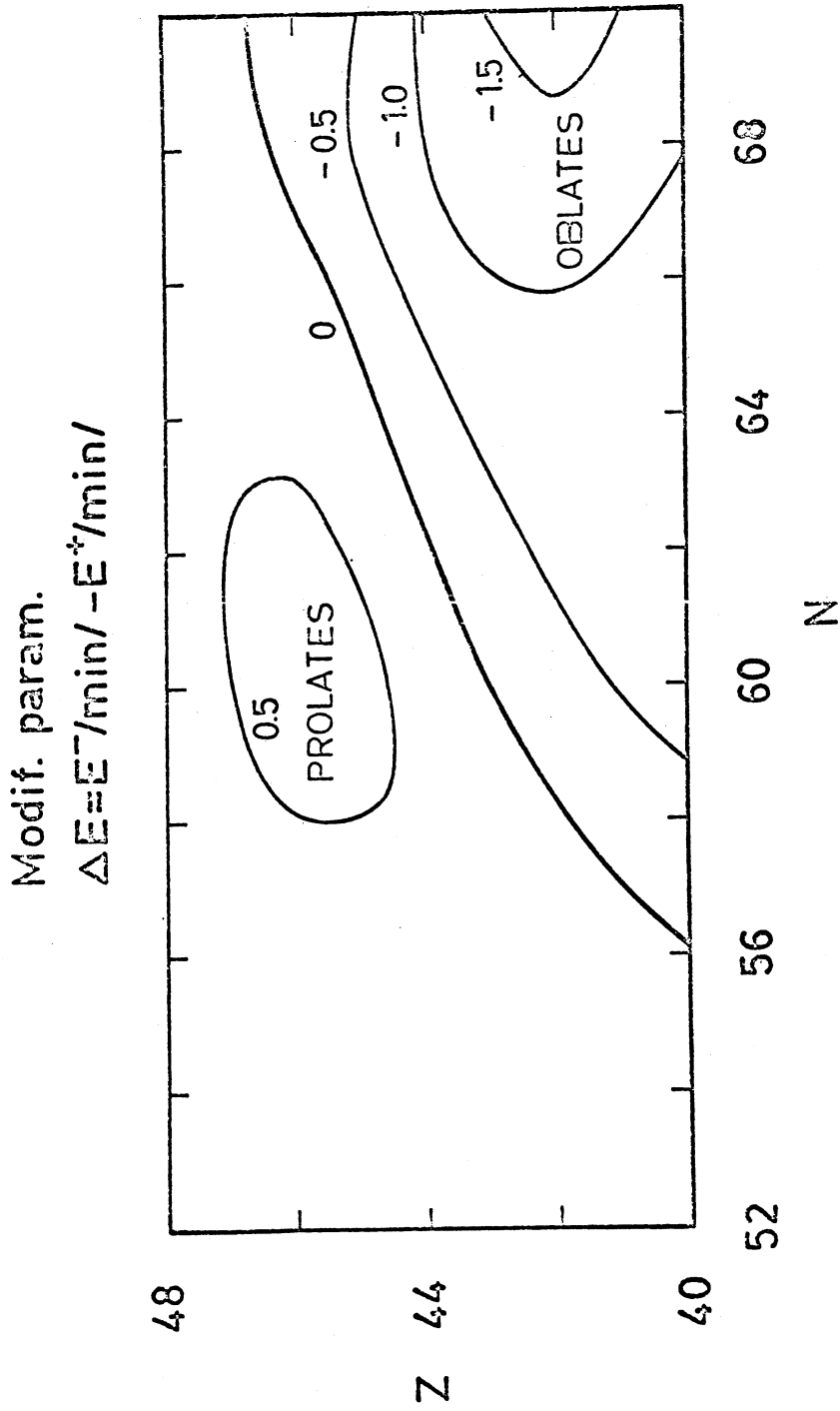


Fig. 6d Same as fig. 6c for the modified parameters.

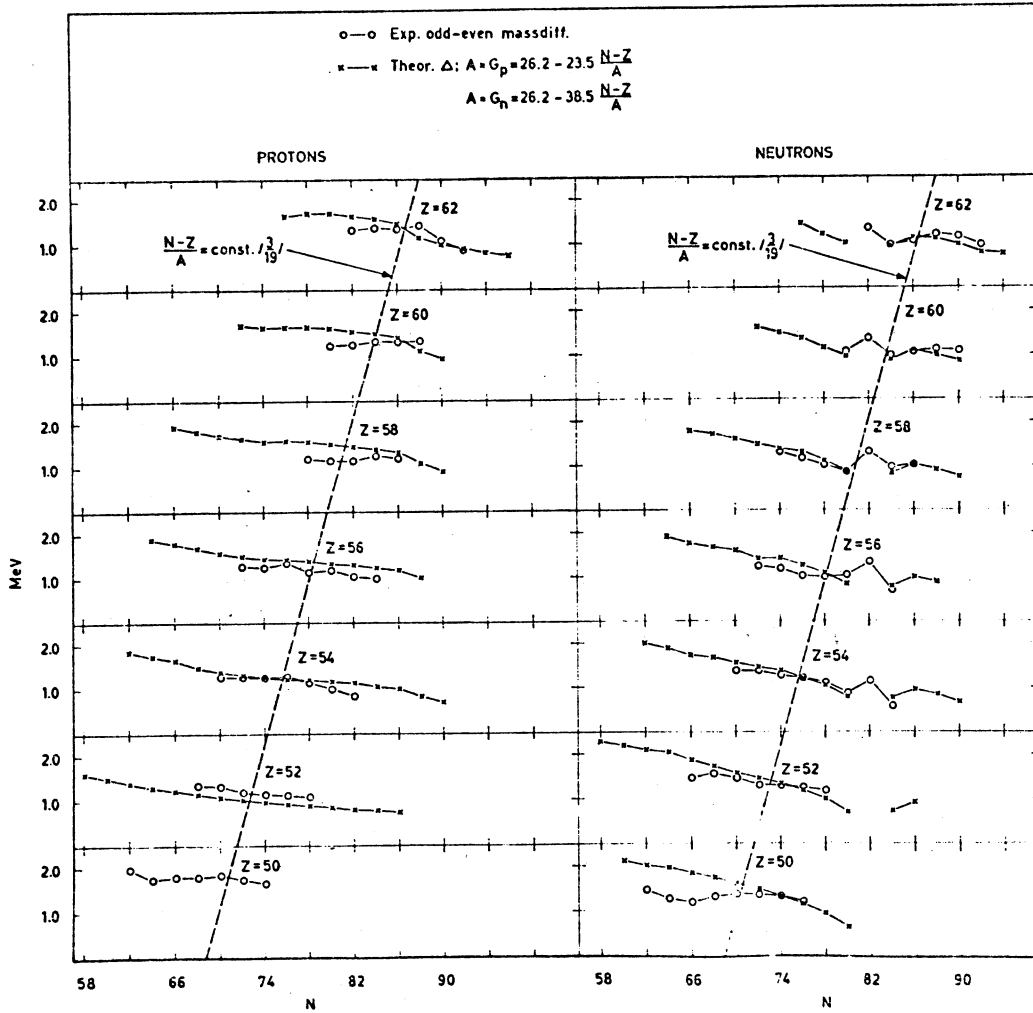


Fig. 7a Experimental odd-even mass differences and calculated  $\Delta$  values. The G values as shown in the figure are those used together with the linearly extrapolated  $\kappa$  and  $\mu$  in the calculations.



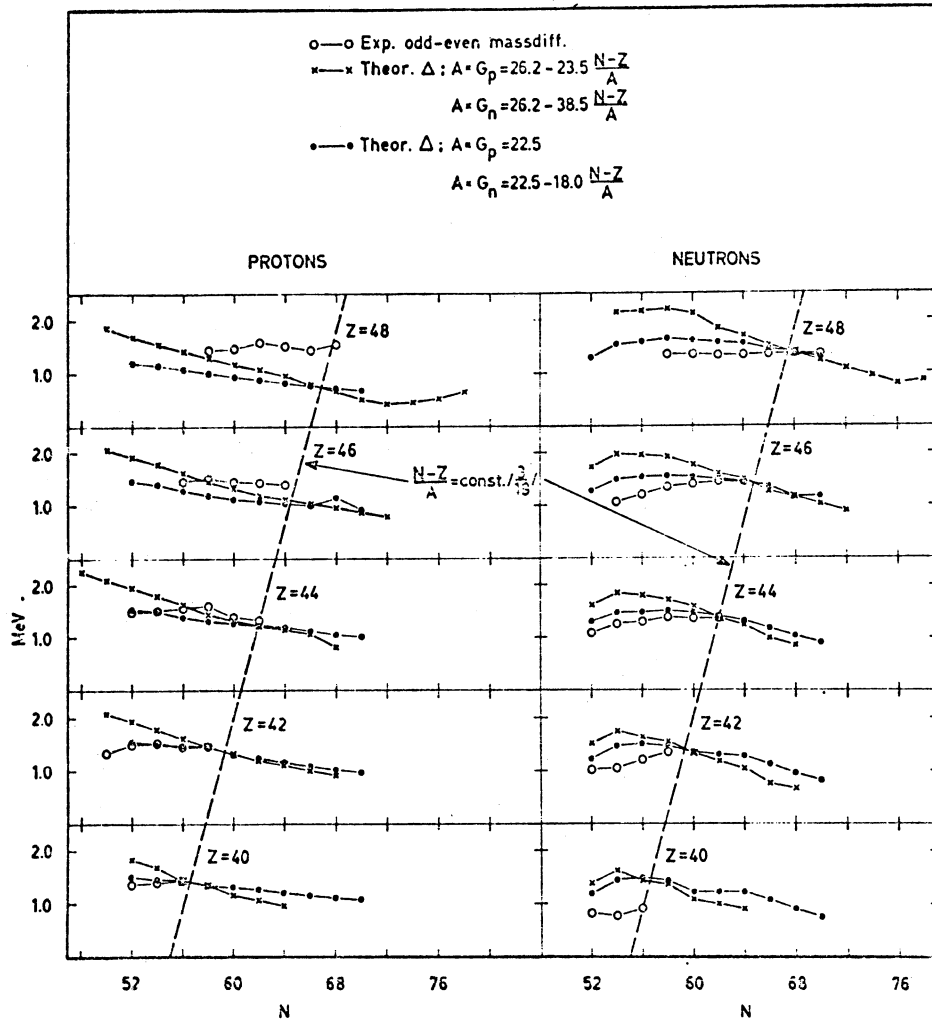


Fig. 7b Same as fig. 7a. The crosses represent the  $\Delta$  values obtained for the G values used together with the linearly extrapolated  $\kappa$  and  $\mu$ , the points correspond to the G values used together with the modified  $\kappa$  and  $\mu$ .

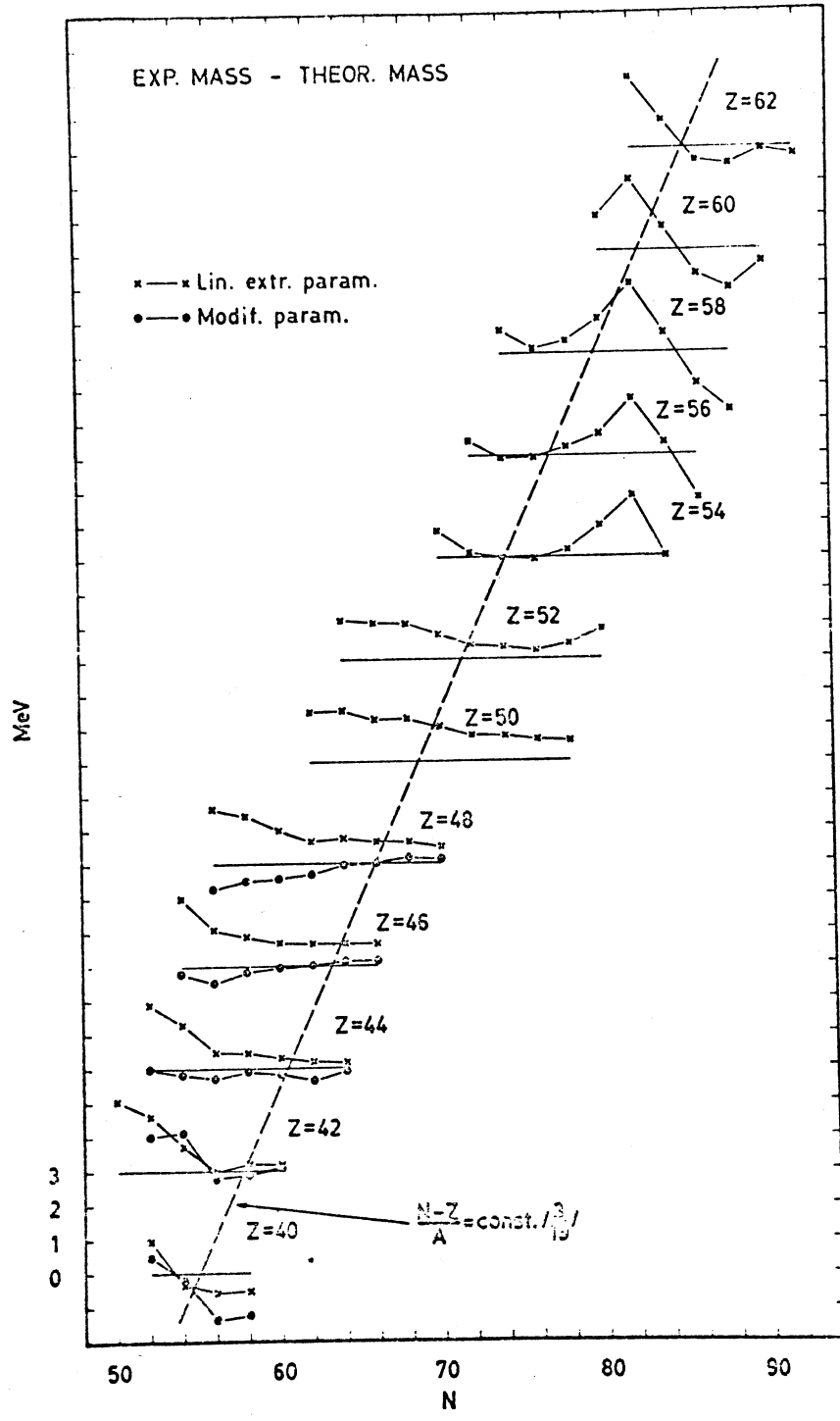


Fig. 8 The difference between the experimental and theoretical masses. The crosses is the fit achieved when  $\kappa$  and  $\mu$  are linearly extrapolated while modified  $\kappa$  and  $\mu$  parameters are associated with the points.

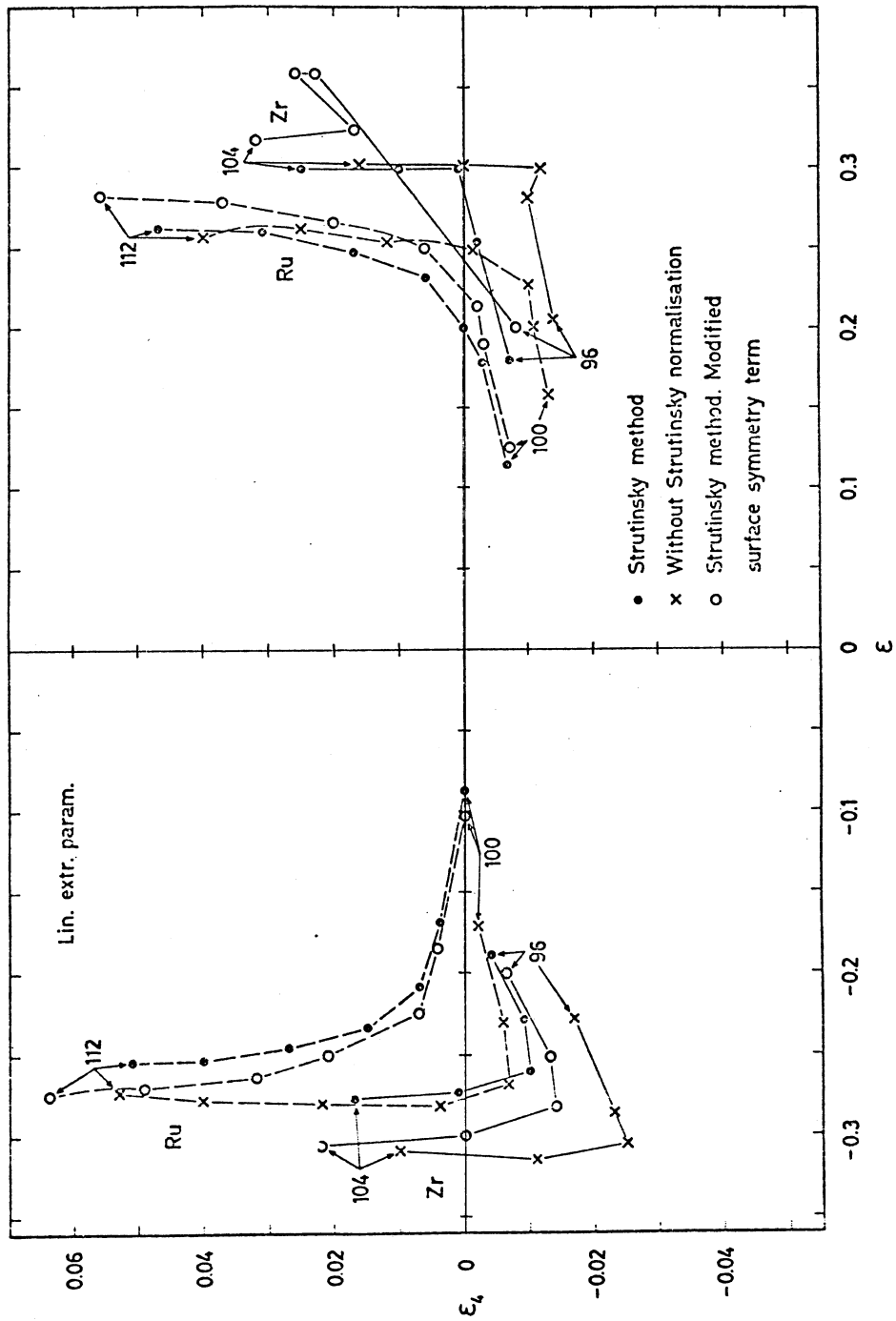


Fig. 9 The minima of the total energy plotted in the  $(\epsilon, \epsilon_4)$ -plane. Linearly extrapolated  $\kappa$  and  $\mu$  values have been used. The points indicate the same minima as fig. 5b, the crosses are obtained when the Bés-Szymanski method is used and the circles when the Myers-Swiatecki isospin dependent surface energy<sup>8)</sup> term is increased by a factor 3 and the Strutinsky method is used.

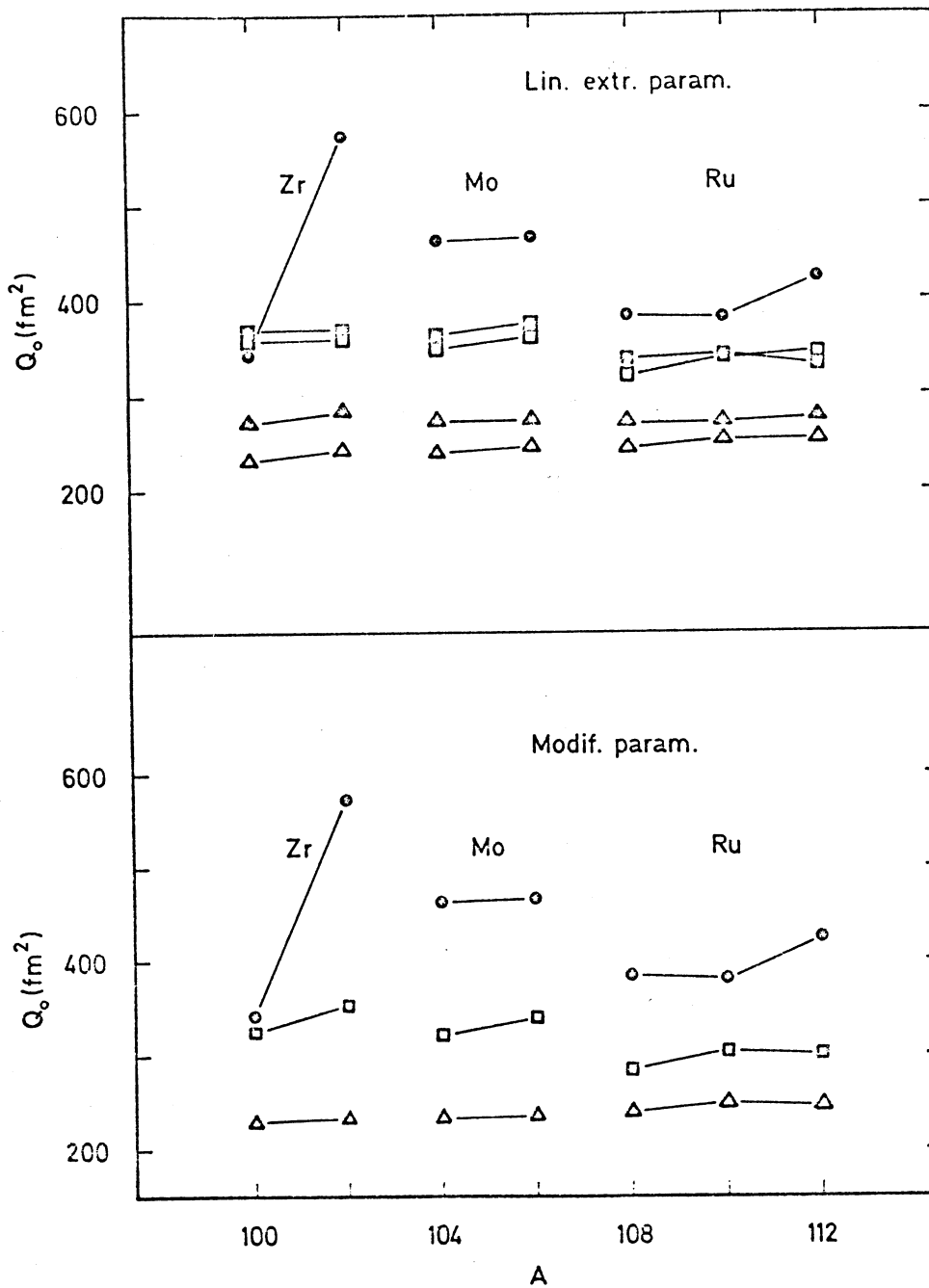


Fig. 10 The experimental intrinsic quadrupole moment, indicated by points<sup>7)</sup>, compared to theoretical results. In the upper part of the figure the linearly extrapolated  $\kappa$  and  $\mu$  values are used, in the lower the modified values. The squares are the quadrupole moments corresponding to the prolate minima, the triangles are associated with the oblate minima. If a square or triangle is open, the Strutinsky method has been used, if it is filled, the Bés-Szymanski method has been used.